ELSEVIER

Journal of Hazardous Materials B137 (2006) 952–958

Journal of Hazardous Materials

www.elsevier.com/locate/jhazmat

Synthesis of nano titania particles embedded in mesoporous SBA-15: Characterization and photocatalytic activity

Jun Yang [a,*], Jun Zhang [a], Liwei Zhu [a], Shaoyuan Chen [a], Yuanming Zhang [a], Yu Tang [a], Yulei Zhu [a,b], Yongwang Li [b]

[a] *Department of Chemistry, Jinan University, Guangzhou 510632, People's Republic China*

[b] *State Key Laboratory of Coal Conversion, Institute of Coal Chemistry, Chinese Academy of Sciences, Taiyuan 030001, People's Republic China*

Received 24 January 2006; received in revised form 6 March 2006; accepted 8 March 2006
Available online 18 April 2006

Abstract

Supported nanocrystalline titanium dioxide (TiO_2) has been prepared by a post-synthesis step via Ti-alkoxide hydrolysis through the use of mesoporous SBA-15 silica. TiO_2/SBA-15 composites with various TiO_2 loading have been prepared and characterized by X-ray diffraction, nitrogen adsorption, Fourier transform infrared spectroscopy and diffusive reflective UV–vis spectroscopy. The addition of mesoporous SBA-15 prevents the anatase to rutile phase transformation and the growth of crystal grain. TiO_2 did not block the SBA-15 pores, and their surface was fully accessible for nitrogen adsorption. Calcination in air of the composites up to 800 °C did not change the nanocrystal phase and slightly increased the domain size from 5.0 to 7.5 nm, indicating that the anatase TiO_2 grains in the mesostructures have a relatively high thermal stability and proper pore diameter allows controlling the size of obtained titania particles. The TiO_2/SBA-15 composites prepared by this study showed much higher photodegradation ability for methylene blue (MB) than commercial pure TiO_2 nanoparticles P-25. Experimental results indicate that the photocatalytic activity of titania/silica mixed materials depends on the adsorption ability of composite and the photocatalytic activity of the titania, and there is an optimal ratio of Ti:Si, too high or low Ti:Si ratio will lower the photodegradation ability of the composites.

Keywords: Nanocrystalline titanium dioxide; Photocatalysis; Mesoporous silica; Methylene blue

1. Introduction

Metal oxide semiconductors, such as TiO_2, ZnO, ZnS and SnO_2, have been applied as photocatalysts for the removal of highly toxic and non-biodegradable pollutants commonly present in air and wastewater [1,2]. Among them titania is believed to be the most promising one, because of its high photocatalytic activity, chemical/photocrossion stability, low cost and without risks for the environment or humans [3,4]. The efficiency of some commercial TiO_2, especially P-25 (Degussa), in the treatment of exhaust gas and wastewater contaminated with organic and inorganic pollutants has been fully proved. In order to maximize photoactivity, TiO_2 particles should be small enough to offer a high number of active sites by unit mass [5]. Therefore, in most cases, the samples are ultrafine powders and have large surface area. However, their effective applications are hindered by two serious disadvantages. Firstly, small particles trend to agglomerate into large particles, making against on catalyst performance. Secondly, the separation and recovery of catalyst is difficult [6,7]. For those reasons many researchers have been focused on mesoporous materials supporting titania catalysts, since they do not only take advantage of high surface area but also make the catalyst-recovering stage more facilitated [8,9].

Ordered mesoporous silica with adjusted pore size, ordered frameworks and specific surface area provides wide opportunities for synthesis titania–silica nano-composites. Deposition titanium dioxides onto a large internal surface or incorporation of Ti species into the frameworks could also obtain some new advanced materials take advantage of both TiO_2 (an n-type semiconductor and active catalyst) and SiO_2 (large surface area and high thermal stability), but also exhibit properties that are not found in the single oxide alone, that could be explained as a synergetic effect [10,11]. The methods of synthesizing

* Corresponding author. Tel.: +86 20 85220223; fax: +86 20 85220223.
E-mail addresses: tyangj@jnu.edu.cn, tyangj@126.com (J. Yang).

0304-3894/$ – see front matter © 2006 Elsevier B.V. All rights reserved.
doi:10.1016/j.jhazmat.2006.03.017

titania–silica mixed oxides include grafting titania on silica support and fabricating titania–silica composites. The titania–silica composite is synthesized by homogeneously mixing suitable precursors [12], in which Ti atoms are incorporated in the silica structure during formation of the silica support itself. In contrast, for the former supported oxides, Ti is introduced in a post-synthesis step by which a titanium precursor is deposited onto the silica surface by grafting methods [13,14], precipitation [15], or impregnation followed by solvent evaporation [16,17]. Recently Aronson et al. [18] used $TiCl_4$ in hexane to graft titania clusters into the pores of MCM-41, which was active in the photodegration of rhodamine-6G. Moreover, titanium oxide was inserted into MCM-41 [16], MCM-48 [14], SBA-15 [19–22].

In the present work, we have investigated the synthesis of TiO_2/SBA-15 materials by a post-synthesis step via Ti-alkoxide hydrolysis in the support-isopropanol suspension. The samples with different content of Ti were prepared and followed by heat treatment at different temperatures. The synthesized materials were characterized by various physical techniques. Photocatalytic activity of the samples has been tested use methylene blue as the model pollutant and compared with P-25.

2. Experimental

2.1. Synthesis

SBA-15 materials were synthesized with the block copolymer Pluronic P123 and tetraethyl orthosilicate (TEOS) following published procedures [23]. In a typical preparation, 4.0 g of P123 was dissolved in 30.0 g of water and 120.0 g of 2 M HCl solution with stirring at 35 °C for 3 h. Then 8.50 g of TEOS was added and the resulting solution was stirred at this temperature for 20 h. The mixture was subsequently raised to 80 °C and aged at this temperature overnight without stirring. After filtration and washing, the solid product was dried at 100 °C then calcined in a stream of air at 500, 700 and 900 °C for 5 h, named as SBA-15-500, SBA-15-700 and SBA-15-900, respectively.

The TiO_2/SBA-15 materials were prepared by hydrolysis of titanium tetraisopropoxide (TTIP) into SBA-15 via a sol–gel method. A typical procedure was as follows: SBA-15 (1.0 g) were sonicated in isopropanol, then the required amount of TTIP (volume ratio TTIP:isopropanol of 1:10) was added dropwise to the solution with stirring of 45 min, the resulting mixture was slowly added water (TTIP/water with volumetric ratio of 1/10) to cause the hydrolysis of the TTIP. The stirring was maintained for 2 h to hydrolyze TTIP completely. The as-synthesized materials were recovered by centrifugation, rinsed with deionized water and ethanol, dried at 80 °C overnight and calcined at 500–900 °C for 2 h. Throughout the subsequent discussion, the samples will be named by indicating the titania content, support and calcined temperature: *x*% TiO_2/SBA-15-*t*, where *x*% was the amount of TiO_2 loading by weight and *t* was the calcination temperature. Pure TiO_2 was synthesized under the same conditions without SBA-15 addition, named as 100% TiO_2.

2.2. Characterization

BET surface area, pore volume and average pore diameter of TiO_2–SiO_2 photocatalysts were measured by N_2 physisorption at −196 °C using Micromeritics ASAP 2020 system. Powder XRD patterns of the catalyst samples were determined on a XD-2 powder X-ray diffractometer using Cu Kα radiation of wavelength 0.15406 nm over the scan range $2\theta = 20$–80° for wide angle XRD. Crystallite size was calculated using Scherrer's formula $d = 0.91\lambda/\beta\cos\theta$. The FT-IR spectra were obtained on a Fourier transform infrared spectrometer (Bruker Equinox 55) using KBr pellets. Diffused reflectance UV–vis spectra were recorded on Shimadzu UV-2550 UV–vis spectrophotometer using barium sulfate as standard.

2.3. Photocatalytic reactions

The photodegradation of MB was performed in order to evaluate the photocatalytic activity of prepared titania/silica materials. The experiments were carried out in a cylindrical double wall jacket glass reactor containing 100 ml of MB solution with an initial concentration of 40 mg/l. The mixture was first stirred for 15 min in dark at room temperature to assure the adsorption equilibrium was reached, then the reaction solution was placed perpendicularly to a 125 W medium pressure mercury lamp by water cooled, and the solution was bubbled with air under magnetic agitation. Commercial pure TiO_2 nanoparticles (P-25, Degussa Co., Germany) 30.0 mg were used for this experiment and the amount of TiO_2/SiO_2 materials necessary to achieve the same TiO_2 loading. The comparison of tested catalysts was done at this fixed TiO_2 concentration because in our experimental conditions, only the semiconductor particles were expected to show photocatalytic activity. Suspension samples of 5 ml volume were collected at fixed time intervals, following centrifugation and the concentration of MB was determined by UV–vis spectrophotometry.

3. Results and discussion

3.1. Textural properties

The specific surface area, pore volumes, average pore sizes and average TiO_2 crystal sizes of P-25, SBA-15 support and TiO_2/SBA-15 samples are listed in Table 1. It can be seen that for *x*% TiO_2/SBA-15-700 °C samples, the BET surface area and the pore volumes decrease with the increase of TiO_2 loading. These results indicate that a part of TiO_2 particles disperse into the pores of SBA-15, leading to decreasing in pore volume and BET surface area. Whereas the average pore diameters increase, which may be probably attributed to an increased contribution of the naked titania character in the samples with the increasing of TiO_2 loading [24]. For TiO_2/SBA-15 samples containing 30% TiO_2 (30% TiO_2/SBA-15-*t*), the BET surface area and the pore volumes decrease with the increase of calcination temperature, whereas the average pore diameters increase, which maybe due to that the nanoparticles trend to agglomerate intensively in the high temperature and the higher calcination temperature could

Table 1
Textural properties and average TiO_2 crystal size of the supported photocatalysts

Catalyst	BET surface area (m^2/g)	Structure	Pore volume (cm^3/g)	Average pore diameter (nm)	Average crystal size (Anat. nm)
P-25	54.0	Anatase/rutile	–	–	21
As-synthesized SBA-15	714.5	–	0.74	4.15	–
SBA-15-700	581.4		0.65	3.89	
SBA-17-900	423.5		0.57	3.68	
30% TiO_2/SBA-15-500	561.0	Anatase	0.55	3.91	–
30% TiO_2/SBA-15-600	504.2	Anatase	0.53	4.17	5.0
30% TiO_2/SBA-15-700	365.1	Anatase	0.41	4.52	7.2
30% TiO_2/SBA-15-800	330.6	Anatase	0.39	4.76	7.5
30% TiO_2/SBA-15-900	298.2	Anatase/rutile	0.31	5.12	8.0
20% TiO_2/SBA-15-700	499.4	Anatase	0.52	4.19	–
40% TiO_2/SBA-15-700	376.1	Anatase	0.45	4.75	6.2
60% TiO_2/SBA-15-700	261.3	Anatase	0.33	5.00	10.5
80% TiO_2/SBA-15-700	142.5	Anatase	0.24	6.64	14.6
100% TiO_2-700	11.3	Almost rutile	0.044	14.34	34.2

make the pore collapsed. When the titania/SBA-15 composites were synthesized by post-synthetic method, the titanium species would be react with surface hydroxyl of the walls in a random fashion, as a consequence, as the content of the TiO_2 increases, the BET surface area and pore volume of the titania/SBA-15 composites decrease.

3.2. XRD

The XRD patterns of 30% TiO_2/SBA-15 samples calcined at different temperatures were shown in Fig. 1. The patterns evidenced that anatase was the only titania crystalline phase in the temperature range of 500–800 °C. As the temperature increased, the peaks of anatase phase became stronger and shaper, and the grain size was determined from the width at half maximum of the anatase (1 0 1) peak according to the Scherrer formula [25] (Table 1). The gradual transformation of anatase phase to rutile phase occurred at 900 °C, whereas 100% TiO_2 calcined at 700 °C anatase phase almost transferred to rutile phase with an

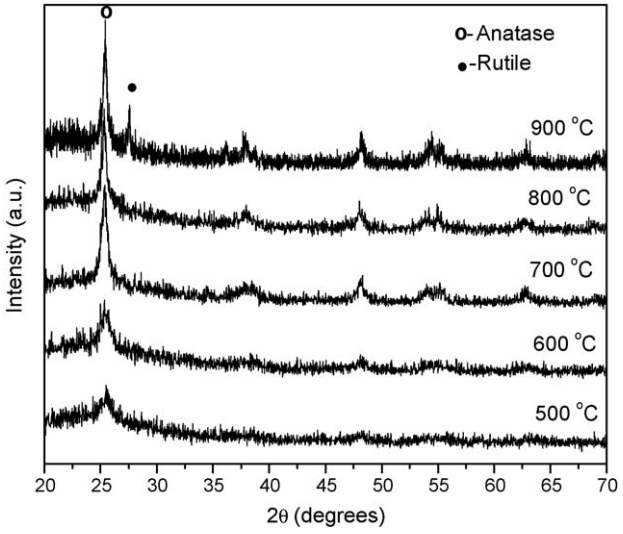

Fig. 1. XRD patterns of 30% TiO_2/SBA-15 calcined at different temperatures.

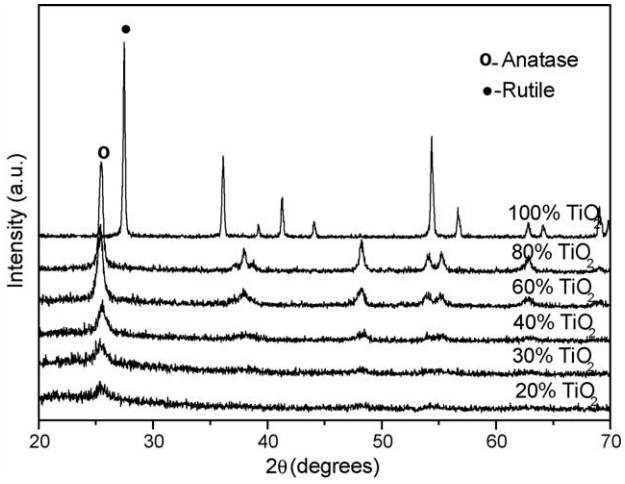

Fig. 2. XRD patterns of TiO_2 supported on SBA-15 with different of TiO_2 contents. (All the samples shown here were calcined at 700 °C.)

average crystal size of 34.2 nm. It strongly suggested that the silica inhibited the formation of rutile phase and the growth of crystal grain. Moreover, the crystalline size of the samples changed slightly during calcination treatment, indicating that the anatase TiO_2 grains in the mesostructures have a relatively high thermal stability. Therefore, this high thermal stability could make it possible to calcine the TiO_2/SiO_2 composites at higher temperature without formation of rutile phase, and to prepare the nanoparticles with high crystallinity and reducing the agglomeration.

The XRD patterns of TiO_2 supported on SBA-15 with TiO_2 content range of 20–100 wt.% were shown in Fig. 2. Along with the decrease in silica content, the (1 0 1) reflection due to anatase was found to increase. These results are in agreement with Cheng and co-workers' report [16], in which titania modified NaY, Na-mordenite zeolites and MCM-41 were prepared by impregnation method.

3.3. FT-IR

FT-IR spectra of the samples calcined at 700 °C for 2 h were shown in Fig. 3. In all spectra, the bands at about 3437

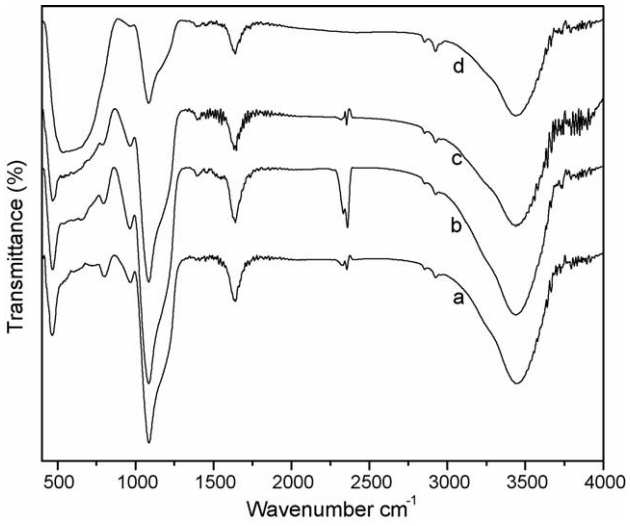

Fig. 3. FT-IR spectra of samples. (a) SBA-15; (b) 30% TiO_2/SBA-15-700 °C; (c) 40% TiO_2/SBA-15-700 °C; (d) 80% TiO_2/SBA-15-700.

and 1636 cm^{-1} can be attributed to the stretching vibration of hydroxyl and water, respectively [26]. It has been reported that adsorbed water, which is probably due to humid KBr and incorporated humidity in the process of sample preparation, has two bands around 3400 and 1630 cm^{-1} [27,28], while Ti–OH bonding presents three bands around 3563, 3172 and 1600 cm^{-1} [29]. Moreover, silanol bonds show absorption at 1450 and 1595 cm^{-1} [30], and small crystallites could result in two broad peaks around 3400 and 1650 cm^{-1} [29]. Ti–O–Ti vibration appeared in the range of 400–600 cm^{-1}. The peak at 1104 cm^{-1} corresponded to the asymmetric stretching vibration of Si–O–Si and the bands at 800 and 470 cm^{-1} can be assigned to the symmetric stretching and deformation modes of Si–O–Si [31], respectively. Theoretically, the IR band observed at 910–960 cm^{-1} might be assigned to the Ti–O–Si stretching vibration [32,33]. As shown in the spectra, a weak band at about 960 cm^{-1} was observed for all samples. For parent SBA-15 silica, this peak was attributed to the Si–OH stretching vibration [34,35]. For TiO_2/SBA-15 samples, this peak indicated the possibility of formation of bonds of Ti–O–Si, and the peak intensity of 30% TiO_2/SBA-15 was obviously higher than that of parent SBA-15.

3.4. Diffusive reflective UV–vis spectroscopy

The UV–vis spectra for TiO_2/SBA-15 samples with different TiO_2 loading are shown in Fig. 4. It can be clearly seen that there is a blue shift in the absorption band edge with the decreasing of TiO_2 content, which can be contributed to the well-known quantum size effect [36]. This is consistent with the results of average crystal size (Table 1). Compared with P-25, absorption band edges of all TiO_2/SBA-15 samples are significantly blue-shifted from the band edge of 380 nm for P-25, which implies a smaller anatase crystallite size for TiO_2/SBA-15 samples. This result strongly suggests that the addition of SBA-15 can effectively suppress the growth of TiO_2 particles.

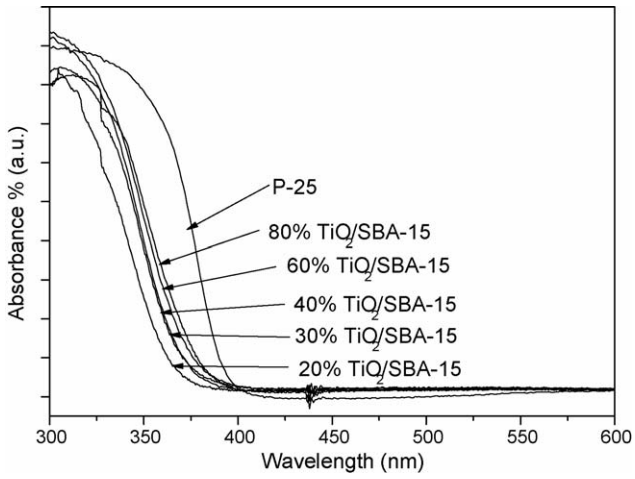

Fig. 4. Diffused reflectance UV–vis spectra of P-25 and TiO_2/SBA-15 composites with different TiO_2 loading. (All samples were calcined at 700 °C.)

3.5. Photodegradation activity

Methylene blue (MB), a basic dye and aromatic pollutants like phenol and toluene, was employed to evaluate the photocatalytic activity of prepared titania/silica materials.

MB could be mineralized into harmless gaseous CO_2, inorganic SO_4^{2-}, NH_4^+ and NO_3^-. First, the central imino-group undergoes a N=C double bond deavage induced by the cleavage of the double bond of $-S^+=$ group in para position in the central aromatic ring. Then the saturation of the two amino bonds yields substituted aniline. Benzene monosulfonic acid and phenol were yielded with the oxidizing reaction going. These masses were finally oxidized into carbon dioxide, inorganic ion and water. More detailed studies on the MB reaction mechanism have been published by several authors, for example, Houas et al. [37] and Gnaser et al. [38].

In photodegradation experiments, there are two factors resulting in the decreasing of the concentration of MB: the adsorption of the MB onto the surface of photocatalyst and the photodegra-

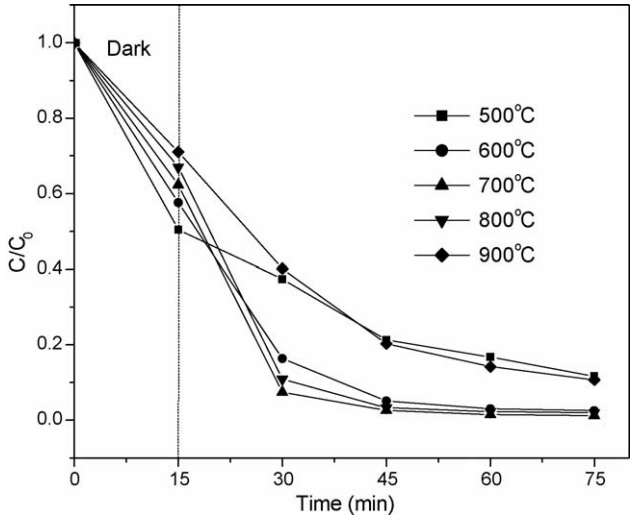

Fig. 5. The photocatalytic activity of the 30% TiO_2/SiO_2 samples calcined at different temperatures.

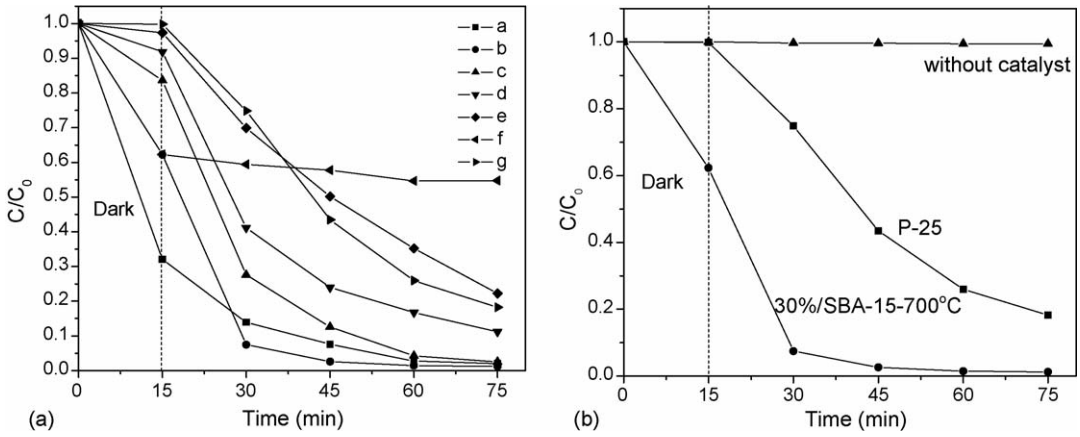

Fig. 6. The photocatalytic performance of the TiO_2/SBA-15 samples with different TiO_2 content: (a) 20% TiO_2; (b) 30% TiO_2; (c) 40% TiO_2; (d) 60% TiO_2; (e) 80% TiO_2; (f) 30% TiO_2/SBA without photo irradiation; (g) P-25; and without catalyst.

dation of MB. Fig. 5 shows the degradation curves of MB by the 30% TiO_2/SBA-15 samples calcined at different temperatures. Fig. 6 shows the degradation curves of MB by the TiO_2/SBA-15 samples with different content of TiO_2 and commercial TiO_2 P-25. For 30% TiO_2/SBA-15-700 °C without UV irradiation (Fig. 6), during the initial 15 min the concentration of MB rapidly decreased and 37.8% of MB decolored, which was due to the adsorption of MB on catalyst surface. After that, the concentration of MB remains almost unchanged, indicating that the adsorption of MB reaches equilibrium. In the absence of irradiation (Figs. 5 and 6) the TiO_2/SBA-15 samples exhibit a much higher adsorption capability of MB than P-25 titania, which is attributed to their much higher specific surface area and pore volumes than pure titania. Furthermore, the TiO_2/SBA-15 samples which have higher surface area exhibit better adsorption capability to MB. Catalyst 20% TiO_2/SBA-15-700 °C has the highest specific surface area of 499.4 m^2/g and the highest adsorption capacity of 67.8% for MB.

In order to get the accurate kinetic data, kinetic experiment were carried out after 15 min dark reaction to assure the adsorption equilibrium was reached. It is well-known that photocatalytic oxidation of organic pollutants follows Langmuir–Hinshelwood kinetics [39,40]. This kind of reaction can be represented as follows:

$$-\frac{dC}{dt} = kt$$

In addition, it can be integrated as follows:

$$kt = \ln\left(\frac{C_0}{C}\right)$$

Where C_0 is the initial concentration of the MB solution and k is a rate constant. The apparent rate constants of different photocatalysts were calculated and listed in Table 2. It can be clearly seen that the addition of SBA-15 significantly improve the photodegradation activity of the catalysts. Catalyst 30% TiO_2/SBA-15-700 has the highest rate constant of 0.0637 min^{-1}, which is much higher than that of P-25 (0.0297 min^{-1}), whereas, 100% TiO_2-700 has the lowest rate constant of 0.0184 min^{-1}. It is generally accepted that for effective degradation, the organic material should be concentrated at the TiO_2 surface firstly, and the large surface area of TiO_2/SBA-15 samples also can adsorb significant amounts of water and hydroxyl groups, which could react with photoexcited holes on the catalyst surface and produce hydroxyl radicals [41]. Furthermore, stable mesostructures and long range ordered with a microporous network of the SBA-15 structure [42] can promote diffusion of reactants and products, enhancing the activity by facilitating access to reactive sites of TiO_2 [43]. In present work, the photoactivity of TiO_2/SBA-15 samples decreased as the following order: 700 °C > 800 °C > 600 °C > 900 °C > 500 °C. TiO_2/SBA-15 calcined at 500 °C has the highest adsorption ability for MB, but its photodegradation ability for MB was much lower than those calcined at 600–800 °C. It is well-known that besides the adsorption ability of catalyst, other factors, such as crystal phase, surface

Table 2
Rate constant of TiO_2/SBA-15 samples and P-25 for MB photodegradation

Catalyst	Rate constant (min^{-1})	Catalyst	Rate constant (min^{-1})
30% TiO_2/SBA-15-500	0.0249	20% TiO_2/SBA-15-700	0.0476
30% TiO_2/SBA-15-600	0.0531	40% TiO_2/SBA-15-700	0.0592
30% TiO_2/SBA-15-700	0.0637	60% TiO_2/SBA-15-700	0.0341
30% TiO_2/SBA-15-800	0.0573	80% TiO_2/SBA-15-700	0.0243
30% TiO_2/SBA-15-900	0.0321	100% TiO_2-700	0.0184
		P-25	0.0297

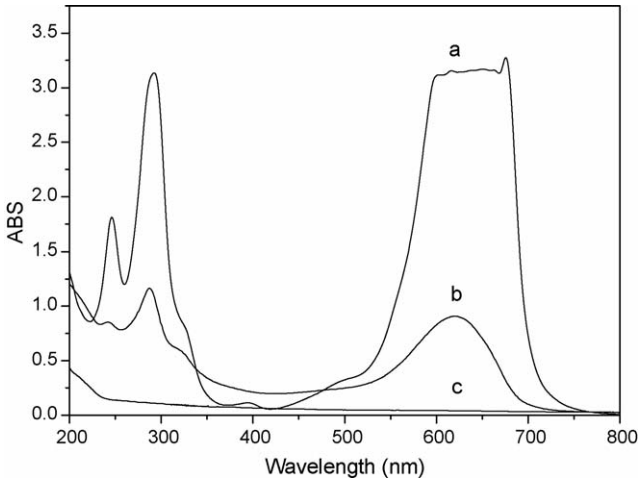

Fig. 7. The UV–vis spectrum of MB by photocatalysis under UV-irradiation after 60 min: (a) 40 mg/l MB; (b) P-25; (c) 30% TiO_2/SBA-15-700 °C.

area, crystallite size and crystallinity, etc. also play an important role in influencing photoactivity. As above results shown (Fig. 1; Table 1), the sample calcined at 500 °C has the highest BET surface area and smallest particle size, but its crystallinity is worse than those calcined at higher temperature, leading to low photoactivity.

For *x*% TiO_2/SBA-15-700 °C photocatalysts with different content, their photocatalytic activities obey the following order: 30% TiO_2 > 40% TiO_2 > 20% TiO_2 > 60% TiO_2 > P-25 > 80% TiO_2 > 100% TiO_2. It is observed that the 30% TiO_2/SBA-15-700 °C sample exhibits the most excellent photocatalytic activity, whereas 20% TiO_2/SBA-15-700 °C sample shows much lower activity even if it has the highest adsorption ability (67.8% MB). The results indicate that the photocatalytic activity of titania/silica mixed materials depends on the adsorption ability of composite and the photocatalytic activity of the titania. There is an optimal ratio of Ti:Si, when the mass ratio of Ti:Si is large, the small TiO_2 particles on the mesoporous silica will easily aggregate to form larger particles (Fig. 2), leading to decrease the photocatalytic activity. On the other hand, when the mass ratio of Ti:Si is small, each nano TiO_2 particle is surrounded by a larger amount of mesoporous silica, which leads to the increase of the average distance from the photoactive sites to the adsorption sites. This situation decreases the efficiency of the photogenerated oxidizing radicals move to the adsorbed pollutants, which leads to decrease of the photocatalytic activity. These results strongly suggest that in order to synthesize the high photocatalytic activity TiO_2/silica composites, there are several factors to be considered, the surface area, the mesoporous structure, the degree of the crystallinity of the titania and the ratio of Ti/Si.

In order to compare the degradation ability of 30% TiO_2/SBA-15 with that of P-25, the UV–vis spectra of 40 mg/l MB solution were measured after 60 min UV radiation in the presence of catalysts, and results are shown in Fig. 7. It can be clearly seen that the degradation ability of titania modified SBA-15 samples prepared by this study were higher than that of commercial pure TiO_2 nanopaticles P-25. There is no absorption band is observed for 30% TiO_2/SBA-15 in the region of 250–700 nm, while P-25 has two broad absorption bands at 280 and 630 nm, respectively. This may be due to several advantages: firstly, the much higher specific surface area and pore volume of the TiO_2/SBA-15 composites than pure titania, which results in high adsorption capability of organic pollutants; secondly, the nice mesoporous structure and more accessible photo-oxidative sites than pure titania, which improves the efficiency of the adsorbed pollutants diffusing to the photo-oxidative sites; thirdly, the smaller particle size of titania with higher crystallization, which leads to improvement of its photocatalytic activity.

4. Conclusion

Nanocrystalline TiO_2/SBA-15 materails had been prepared by a post-synthesis step via Ti-alkoxide hydrolysis in the support-isopropanol suspension and characterized by several physical techniques. The dispersion effect promoted by mesoporous SBA-15 prevents the anatase to rutile phase transformation and the growth of crystal grain. Moreover, the crystalline size of the samples changes slightly upon calcinations treatment, indicating that the anatase TiO_2 grains in the mesostructures have a relatively high thermal stability and proper pore diameter allows controlling the size of obtained titania particles. The titania modified SBA-15 samples prepared by this study showed much higher photodegradation ability for MB than commercial pure TiO_2 P-25.

Acknowledgements

We gratefully acknowledge financial support from the Team Project of Guangdong Province Natural Science Foundation (Grant No. 05200555) and National Ministry of Science and Technology of China via 863 plan (Project No. 2001AA523010).

References

[1] M.A. Fox, M. Dulay, Heterogeneous photocatalysis, Chem. Rev. 93 (1993) 341.
[2] M.R. Hoffmann, S.T. Martin, W.Y. Choi, D.W. Bahnemann, Environmental applications of semiconductor photocatalysis, Chem. Rev. 95 (1995) 69.
[3] O. Legrini, E. Oliveros, A.M. Braun, Photochemical processes for water treatment, Chem. Rev. 93 (1993) 671.
[4] O. Carp, C.L. Huisman, A. Reller, Photoinduced reactivity of titanium dioxide, Prog. J. Solid State Chem. 32 (2004) 33.
[5] Z. Zhang, C.C. Wang, R. Zakaria, J.Y. Ying, Role of particle size in nanocrystalline TiO_2-based photocatalysts, J. Phys. Chem. B 102 (1998) 10871.
[6] Y. Zhu, L. Zhang, W. Yao, L. Cao, The chemical states and properties of doped TiO_2 film photocatalyst prepared using the sol–gel method with $TiCl_4$ as a precursor, Appl. Surf. Sci. 158 (2000) 32.
[7] J.C. Yu, J.G. Yu, J.C. Zhao, Enhanced photocatalytic activity of mesoporous and ordinary TiO_2 thin films by sulfuric acid treatment, Appl. Catal. B: Environ. 36 (2002) 31.
[8] H. Yamashita, S. Kawasaki, Y. Ichihashi, M. Harada, M. Takeuchi, M. Anpo, Characterization of titanium–silicon binary oxide catalysts prepared by the sol–gel method and their photocatalytic reactivity for the liquid-phase oxidation of 1-octanol, J. Phys. Chem. B 102 (1998) 5870.
[9] X. Fu, L.A. Clark, Q. Yang, M.A. Anderson, Enhanced photocatalytic performance of titania-based binary metal oxides: TiO_2/SiO_2 and TiO_2/ZrO_2, Environ. Sci. Technol. 30 (1996) 647.

[10] P. Cheng, M.P. Zheng, Y.P. Jin, Q. Huang, M.Y. Gu, Preparation and characterization of silica-doped titania photocatalyst through sol–gel method, Mater. Lett. 57 (2003) 2989.
[11] C. Minero, F. Catozzo, E. Pelizzetti, Role of adsorption in photocatalyzed reactions of organic molecules in aqueous titania suspensions, Langmuir 8 (1992) 481.
[12] X. Zhang, F. Zhang, K.Y. Chan, Synthesis of titania–silica mixed oxide mesoporous materials, characterization and photocatalytic properties, Appl. Catal. A 284 (2005) 193.
[13] W. Yan, B. Chen, S.M. Mahurin, E.W. Hagaman, S. Dai, S.H. Overbury, Surface sol–gel modification of mesoporous silica materials with TiO_2 for the assembly of ultrasmall gold nanoparticles, J. Phys. Chem. B 108 (2004) 2793.
[14] M. Widenmeyer, S. Grasser, K. Köhler, R. Anwander, TiO_x overlayers on MCM-48 silica by consecutive grafting, Microporous Mesoporous Mater. 44–45 (2001) 327.
[15] A. Hanprasopwattana, S. Srinivasan, A.G. Sault, A.K. Datye, Titania coatings on monodisperse silica spheres (characterization using 2-propanol dehydration and TEM), Langmuir 12 (1996) 3173.
[16] Y.H. Hsien, C.F. Chang, Y.H. Chen, S. Cheng, Photodegradation of aromatic pollutants in water over TiO_2 supported on molecular sieves, Appl. Catal. B 31 (2001) 241.
[17] A.A. Belhekar, S.V. Awate, R. Anand, Photocatalytic activity of titania modified mesoporous silica for pollution control, Catal. Commun. 3 (2002) 453.
[18] B.J. Aronson, C.F. Blanford, A. Stein, Solution-phase grafting of titanium dioxide onto the pore surface of mesoporous silicates: synthesis and structural characterization, Chem. Mater. 9 (1997) 2842.
[19] A. Tuel, L.G. Hubert-Pfalzgraf, Nanometric monodispersed titanium oxide particles on mesoporous silica: synthesis, characterization, and catalytic activity in oxidation reactions in the liquid phase, J. Catal. 217 (2003) 343.
[20] F. Chiker, J.Ph. Nogier, F. Launay, J.L. Bonardet, New Ti-SBA mesoporous solids functionnalized under gas phase conditions: characterisation and application to selective oxidation of alkenes, Appl. Catal. A 243 (2003) 309.
[21] Z. Luan, J.Y. Bae, L. Kevan, Photoionization of *N*-alkylphenothiazines in tianosilicate mesoporous TiSBA-15 molecular sieves, Micropor. Mesopor. Mater. 48 (2001) 189.
[22] M.V. Landau, L. Vradman, Xueguang Wang, L. Titelman, High loading TiO_2 and ZrO_2 nanocrystals ensembles inside the mesopores of SBA-15: preparation, texture and stability, Micropor. Mesopor. Mater. 78 (2005) 117.
[23] D.Y. Zhao, Q. Huo, J. Feng, B.F. Chmelka, G.D. Stucky, Nonionic triblock and star diblock copolymer and oligomeric surfactant syntheses of highly ordered, hydrothermally stable, mesoporous silica structures, J. Am. Chem. Soc. 120 (1998) 6024.
[24] Y.X. Chen, L.P. Xu, Y.Z. Wang, C.G. Gao, D.S. Liu, Preparation of Ti–Si mixed oxides by sol–gel one step hydrolysis, Catal. Today 93–95 (2004) 583.
[25] H.P. Klug, L.E. Alexander, X-ray Diffraction Procedures, Wiley, New York, 1954.
[26] M. Guidotti, N. Ravasio, R. Psaro, G. Ferraris, G. Moretti, Epoxidation on titanium-containing silicates: do structural features really affect the catalytic performance? J. Catal. 214 (2003) 242.
[27] Y. Suda, T. Morimoto, Molecularly adsorbed water on the bare surface of titania (rutile), Langmuir 3 (1987) 786.
[28] K. Tanaka, J.M. White, Characterization of species adsorbed on oxidized and reduced anatase, J. Phys. Chem. 86 (1982) 4708.
[29] E. Sanchez, T. Lopez, R. Gomez, Bokhimi, A. Morales, O. Novaro, Synthesis and characterization of sol–gel Pt/TiO_2 catalyst, J. Solid State Chem. 122 (1996) 309.
[30] S. Klein, S. Thorimbert, W.F. Maier, Amorphous microporous titania–silica mixed oxides: preparation, characterization, and catalytic redox properties, J. Catal. 163 (1996) 476.
[31] K.Y. Jung, S.B. Park, Enhanced photoactivity of silica-embedded titania particles prepared by sol–gel process for the decomposition of trichloroethylene, Appl. Catal. B 25 (2000) 249.
[32] S. Kein, S. Thorimbert, W.F. Maier, Amorphous microporous titania–silica mixed oxides: preparation, characterization, and catalytic redox properties, J. Catal. 163 (1996) 476.
[33] D.W. Lee, S.K. Ihm, K.H. Lee, Mesostructure control using a titania-coated silica nanosphere framework with extremely high thermal stability, Chem. Mater. 17 (2005) 4461.
[34] Z. Ding, G.Q. Lu, P.F. Greenfield, Role of the crystallite phase of TiO_2 in heterogeneous photocatalysis for phenol oxidation in water, J. Phys. Chem. B 104 (2000) 4815.
[35] T. Blasco, M.A. Camblor, A. Corma, J.P. Pariente, The state of Ti in titanoaluminosilicates isomorphous with zeolite beta, J. Am. Chem. Soc. 115 (1993) 11806.
[36] A. Henglein, Small-particle research: physicochemical properties of extremely small colloidal metal and semiconductor particles, Chem. Rev. 89 (1989) 1861.
[37] A. Houas, H. Lachheb, M. Ksibi, E. Elaloui, C. Guillard, J.M. Herrmann, Photocatalytic degradation pathway of methylene blue in water, Appl. Catal. B 31 (2001) 145.
[38] H. Gnaser, M.R. Savina, W.F. Calaway, C.E. Tripa, I.V. Veryovkin, M.J. Pellin, Photocatalytic degradation of methylene blue on nanocrystalline TiO_2: surface mass spectrometry of reaction intermediates, Int. J. Mass Spectrom. 245 (2005) 61.
[39] Y.Z. Li, S.J. Kim, Synthesis and characterization of nano titania particles embedded in mesoporous silica with both high photocatalytic activity and adsorption capability, J. Phys. Chem. B 109 (2005) 12309.
[40] S.S. Hong, M.S. Lee, S.S. Park, G.D. Lee, Synthesis of nanosized TiO_2/SiO_2 particles in the microemulsion and their photocatalytic activity on the decomposition of *p*-nitrophenol, Catal. Today 87 (2003) 99.
[41] C.S. Turchi, D.F. Ollis, Photocatalytic degradation of organic-water contaminants mechanisms involving hydroxyl radical attack, J. Catal. 122 (1990) 178.
[42] M. Kruk, M. Jaroniec, C.H. Ko, et al., Characterization of the porous structure of SBA-15, Chem. Mater. 12 (2000) 1961.
[43] Z. Shan, E. Gianotti, J.C. Jansen, J.A. Peters, L. Marchese, T. Maschmeyer, One-step synthesis of a highly active, mesoporous, titanium-containing silica by using bifunctional templating, Chem. Eur. J. 7 (2001) 1437.